

Enrichment of Nanofiber Hydrogel Composite with Fractionated Fat Promotes Regenerative Macrophage Polarization and Vascularization for Soft-Tissue Engineering

Dominic Henn, M.D.

Katharina S. Fischer, B.S.

Kellen Chen, Ph.D.

Autumn H. Greco, B.S.

Russell A. Martin, Ph.D.

Dharshan Sivaraj, B.S.

Artem A. Trotsyuk, B.S.

Hai-Quan Mao, Ph.D.

Sashank K. Reddy, M.D., Ph.D.

Ulrich Kneser, M.D.

Geoffrey C. Gurtner, M.D.

Volker J. Schmidt, M.D.

Justin M. Sacks, M.D., M.B.A.

Stanford, Calif.; Heidelberg, Germany;

Baltimore, Md.; Roskilde, Denmark;

and St. Louis, Mo.



Background: Fractionated fat has been shown to promote dermal regeneration; however, the use of fat grafting for reconstruction of soft-tissue defects is limited because of volume loss over time. The authors have developed a novel approach for engineering of vascularized soft tissue using an injectable nanofiber hydrogel composite enriched with fractionated fat.

Methods: Fractionated fat was generated by emulsification of groin fat pads from rats and mixed in a 3:1 ratio with nanofiber hydrogel composite (nanofiber hydrogel composite with fractionated fat). Nanofiber hydrogel composite with fractionated fat or nanofiber hydrogel composite alone was placed into isolation chambers together with arteriovenous loops, which were subcutaneously implanted into the groin of rats ($n = 8$ per group). After 21 days, animals were euthanized and systemically perfused with ink, and tissue was explanted for histologic analysis. Immunofluorescent staining and confocal laser scanning microscopy were used to quantify CD34⁺ progenitor cell and macrophage subpopulations.

Results: Nanofiber hydrogel composite with fractionated fat tissue maintained its shape without shrinking and showed a significantly stronger functional vascularization compared to composite alone after 21 days of implantation (mean vessel count, 833.5 ± 206.1 versus 296.5 ± 114.1 ; $p = 0.04$). Tissue heterogeneity and cell count were greater in composite with fractionated fat (mean cell count, $49,707 \pm 18,491$ versus 9263 ± 3790 ; $p = 0.005$), with a significantly higher number of progenitor cells and regenerative CD163⁺ macrophages compared to composite alone.

Conclusions: Fractionated fat-enriched nanofiber hydrogel composite transforms into highly vascularized soft tissue over 21 days without signs of shrinking and promotes macrophage polarization toward regenerative phenotypes. Enrichment of injectable nanofiber hydrogel composite with fractionated fat represents a promising approach for durable reconstruction of soft-tissue defects. (*Plast. Reconstr. Surg.* 149: 433e, 2022.)

Clinical Relevance Statement: The authors' approach for tissue engineering may ultimately lay the groundwork for clinically relevant applications with the goal of generating large volumes of vascularized soft tissue for defect reconstruction without donor site morbidity.

From the Hagey Laboratory for Pediatric Regenerative Medicine, Division of Plastic and Reconstructive Surgery, Department of Surgery, Stanford University; Department of Hand, Plastic, and Reconstructive Surgery, BG Trauma Center Ludwigshafen, Ruprecht-Karls-University of Heidelberg; Department of Materials Science and Engineering, Whiting School of Engineering, and Institute for NanoBioTechnology, Johns Hopkins University; Translational Tissue Engineering Center and Department of Biomedical Engineering, and Department of Plastic and Reconstructive Surgery, Johns Hopkins School of Medicine; Department for Plastic and Breast Surgery, Zealand University Hospital Roskilde; and Division of Plastic and Reconstructive Surgery, Department of Surgery, Washington University in St. Louis School of Medicine.

Received for publication October 26, 2020; accepted August 18, 2021.

K.S.F. and K.C. contributed equally to this article.

V.J.S. and J.M.S. contributed equally to this article.

Copyright © 2022 by the American Society of Plastic Surgeons
DOI: 10.1097/PRS.00000000000008872

Disclosure: R.A.M., S.K.R., J.M.S., and H.Q.M. are co-inventors of the intellectual property covering the technology that has been filed by Johns Hopkins University and have equity positions in LifeSprout, a privately held company that is seeking to bring these advances into clinical development. The remaining authors have no financial interests to report.

Related digital media are available in the full-text version of the article on www.PRSJournal.com.

Fat grafting has shown regenerative effects in the treatment of several clinical conditions such as diabetic ulcers, irradiated skin, and scar contractures.¹ The therapeutic benefits of fat grafting have been attributed to the presence of adipose-derived stromal cells.^{2,3} Adipose-derived stromal cells contain mesenchymal multipotent stem cells, which are present in the stromal vascular fraction of lipoaspirates and secrete a variety of growth factors, thereby promoting tissue regeneration.⁴ In 2013, Tonnard et al. demonstrated that adipose-derived stromal cells withstand the mechanical emulsification and filtration of lipoaspirates into a liquid suspension for injection into the superficial dermis, termed “nanofat.”⁵ Because of its regenerative properties, nanofat has since been clinically used for the treatment of age-related structural changes of the skin and superficial rhytides of the face.^{5,6} Fractionated fat (or FractoFat) can be generated using a similar emulsification process without filtration and was described by Rohrich et al. to effectively blend the lid-cheek junction, thus providing volume restoration in the periorbital area.⁷

Despite being a valuable tool to induce dermal regeneration and restore volume deficits, fat grafting is mainly limited by the temporary nature of its beneficial effects, often requiring multiple serial applications to achieve the desired outcome.⁸ The reconstruction of defects caused by trauma or tumor resection, however, requires long-lasting and stable volume restoration, which is why autologous flaps remain the clinical gold standard for this indication, despite the risk of significant donor-site morbidity.⁹ To overcome the inherent challenges associated with autologous tissue transfer, our group has developed an injectable hydrogel composed of hyaluronic acid cross-linked with electrospun poly-(ϵ -caprolactone) nanofibers. This nanofiber hydrogel compound displays biomechanical properties similar to adipose tissue, and has also been proven to enable a durable volume restoration.^{10,11} Moreover, the nanofiber hydrogel compound enhances native tissue regeneration and promotes angiogenesis *in vivo*, thus providing an alternative approach for minimally invasive defect reconstruction without the risk for donor-site morbidity.^{10,11}

In this study, we developed a novel approach to enhance the ability of nanofiber hydrogel compound to generate large volumes of vascularized soft tissue by leveraging the regenerative capacity of fractionated fat. The established arteriovenous loop model was used to assess the capacity of the nanofiber hydrogel compound to sustain

a functional vascularization within an isolation chamber, which allows for a precise tissue explanation after a defined period of *in vivo* implantation.^{12,13} Immunofluorescent staining and confocal laser scanning microscopy were used to quantify progenitor cells and analyze the infiltration of macrophages into the neotissue.

MATERIALS AND METHODS

Animals

Operations were performed on 16 female Sprague Dawley rats (Charles River Laboratories, Sulzfeld, Germany), weighing 280 to 320 g, and aged 10 to 14 months. Animals were kept on a 12-hour dark/light cycle and had free access to food and water. Operations were performed under inhalation anesthesia with isoflurane (2.5%) in pure oxygen using a surgical microscope with 16 \times magnification (OPMI pico; Zeiss, Oberkochen, Germany). Heparin (80 IU/kg intravenously) and buprenorphine (0.05 mg/kg subcutaneously; Bayer, Leverkusen, Germany) were administered until postoperative day 2. The animals were euthanized by means of intracardial injection of pentobarbital under deep anesthesia. All animal operations were performed at the research laboratory of the BG Trauma Center Ludwigshafen according to the German Animal Welfare Act and were approved by the Institutional Animal Care and Use Committee of the local governmental authorities (Landesuntersuchungsamt Rheinland-Pfalz G-13-7-008).

Preparation of Nanofiber Hydrogel Composite

To generate the nanofiber hydrogel compound scaffolds, hyaluronic acid was conjugated with acrylate groups, and then cross-linked with polyethylene glycol dithiol to form a hydrogel. In the same step, cryomilled electrospun poly-(ϵ -caprolactone) nanofiber fragments were grafted into the hydrogel network by means of surface-grafted maleimide groups. Poly-(ϵ -caprolactone) is a biodegradable, linear, aliphatic, polyester polymer that degrades *in vivo* through hydrolytic random scission and is cleared without bioaccumulation.^{14,15} The nanofiber hydrogel compound formed after a cross-linking reaction at 37°C overnight. Synthesis and characterization of the nanofiber hydrogel compound have been described previously in detail.¹⁰

Enrichment of Nanofiber Hydrogel Composite with Fractionated Fat

The inguinal fat pad was harvested from the groins of the rats ($n = 8$) and the epigastric vessels

were coagulated. The inguinal fat pad was mechanically emulsified by pushing it 20 times between two 5-cc syringes connected by a Luer-lock connector with 2.4-mm holes (Gems Anaerobic Transfers; Tulip Medical Products, San Diego, Calif.). The fractionated fat was then homogenized with nanofiber hydrogel compound at a 3:1 ratio in a similar fashion using the Tulip Luer-lock connector and two syringes to create the nanofiber hydrogel composite with fractionated fat scaffold (Fig. 1, *above, left*). Transplantation of nanofiber hydrogel composite with fractionated fat was performed autologously into the same animals from which the fat pads had been harvested.

Microsurgical Arteriovenous Loop Creation

The saphenous arteries and veins of both hind limbs were dissected and exposed along the medial thighs of the rats. A 20-mm-long saphenous vein graft was harvested from the left leg and subsequently transferred to the right leg, where an arteriovenous loop was created by means of anastomosis of the vein graft between the right saphenous artery and saphenous vein in an end-to-end fashion using 11-0 Ethilon sutures (Ethicon, Inc., Somerville, N.J.). Observation of pulsatility and the double occlusion test were used to assess patency of the microanastomoses. Arteriovenous loops were placed into round polytetrafluoroethylene isolation chambers (height, 10 mm; inner diameter, 10 mm), which were sealed with a lid (Harhaus Devices, Remscheid, Germany) and sutured onto the underlying muscle fascia (Prolene 6-0; Ethicon). The chamber design has been described previously.¹⁶ The chambers were filled with 0.8 ml of nanofiber hydrogel composite with fractionated fat or an equal amount of nanofiber hydrogel composite alone ($n = 8$ animals per group) (Fig. 1, *above*). Wound closure was performed with running subcutaneous (Vicryl 3-0; Ethicon) and cutaneous sutures (Vicryl 4-0; Ethicon).

Histologic Analysis of Vascularization

Visualization of perfused blood vessels within the scaffolds on postoperative day 21 after arteriovenous loop creation was achieved by means of cannulization of the descending aorta of the rats with a 24-gauge catheter, followed by flushing with heparan solution (100 IU/ml) and 30 ml of warm (37°C) India Ink solution [50% volume/volume India Ink (Windsor & Newton, London, United Kingdom) in 5% gelatin and 4% mannitol]. After explantation from the chambers, the tissue was fixed in 4% paraformaldehyde, and dehydrated

in 30% sucrose in 1× phosphate-buffered saline for at least 48 hours. Tissue was then incubated in optimal cutting temperature compound (O.C.T.; TissueTek, Sakura Finetek, Torrance, Calif.) for 24 hours at 4°C and cryoembedded in tissue molds on dry ice. Frozen sections of 7- μ m thickness were performed on a cryostat perpendicular to the longitudinal arteriovenous loop axis in the central area of the chamber. Hematoxylin and eosin and Masson trichrome staining were performed according to the manufacturer's recommendation (Sigma-Aldrich). Stained cross-sections were visualized with a Zeiss Axio Vision microscope and recorded with the Axio Vision 4 software (Carl Zeiss Microscopy, Jena, Germany). An observer-independent software algorithm in Matlab (Mathworks, Natick, Mass.) specifically developed for quantification of neoangiogenesis in the arteriovenous loop model was used to quantify ink-filled functional blood vessels on histologic cross-sections.¹⁷

Immunofluorescent Staining and Confocal Laser Scanning Microscopy

Antigen retrieval was performed using 0.01 M sodium citrate buffer in phosphate-buffered saline (Abcam, Cambridge, Mass.), followed by blocking for 2 hours in 5% goat serum (Invitrogen, Waltham, Mass.) in phosphate-buffered saline. Sections were incubated in mouse anti-rat CD163 antibody (clone ED2, BioRad, MCA342R), mouse anti-rat CD68 antibody (clone ED1, BioRad, MCA341R), and rabbit anti-CD34 antibody (EP373Y, Abcam, ab81289) diluted 1:100 in 5% goat serum overnight at 4°C. Secondary antibodies were applied for 1 hour at room temperature (Goat anti-Rabbit IgG (H+L) Highly Cross-Adsorbed Secondary Antibody, Alexa Fluor Plus 488; Goat anti-Mouse IgG (H+L) Cross-Adsorbed Secondary Antibody; Thermo Fisher, Waltham, Mass.). Imaging was performed on a Zeiss LSM 880 confocal laser scanning microscope at the Cell Science and Imaging Facility at Stanford University. To obtain high-resolution images of the entire tissue cross-section, multiple images of 25× magnification were taken using automatic tile scanning. Individual images were stitched together during acquisition using the ZEN Black software (Carl Zeiss, Oberkochen, Germany).

Quantification of Immunofluorescent Staining

Immunofluorescent staining was quantified using a code written in Matlab adapted from previous image analysis studies by one of the authors (K.C.).^{18,19} Briefly, confocal images were separated

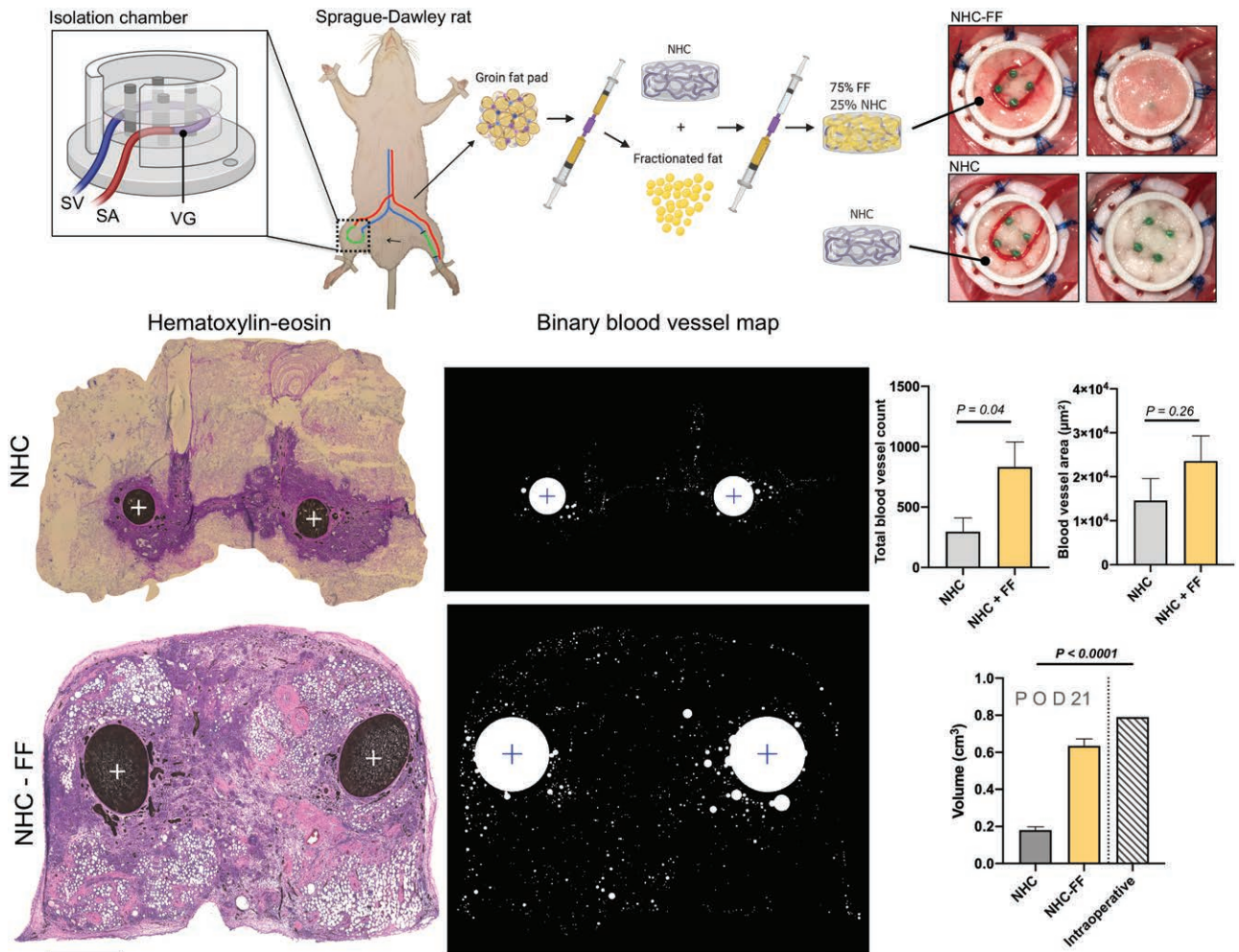


Fig. 1. (Above, left) For creation of an arteriovenous loop, the saphenous artery and vein were dissected and exposed along the medial thigh of Sprague Dawley rats. A 20-mm-long saphenous vein graft was harvested from the left leg (green) and subsequently transferred to the right leg, where an arteriovenous loop was created by means of anastomosis of the vein graft (green) between the right saphenous artery (red) and vein (blue) in an end-to-end fashion. The arteriovenous loop was placed into a round polytetrafluoroethylene isolation chamber and wrapped around the four fixation pins of the chamber to prevent dislocation (inset: SV, saphenous vein; SA, saphenous artery; VG, vein graft). To create autologous fractionated fat grafts, the inguinal fat pad was harvested from the groins of the rats and mechanically emulsified by pushing it 20 times between two 5-cc syringes connected by a Tulip Luer-lock connector. The fractionated fat was then homogenized with nanofiber hydrogel composite (NHC) at a 3:1 ratio in a similar fashion using the Luer-lock connector and two syringes. (Above, right) In one group of rats, the arteriovenous loop was embedded into nanofiber hydrogel composite with fractionated fat (NHC-FF) mixture; the control group received nanofiber hydrogel compound only. (Center, left and below, left) Histologic cross-sections of explanted nanofiber hydrogel composite (center, left) and nanofiber hydrogel composite with fractionated fat remodeled tissue at 21 days after implantation, stained with hematoxylin and eosin. Functional neovessels appear black because of systemic perfusion with India Ink before tissue explantation; +, arteriovenous loop main vessels. (Below, center) Binary blood vessel map created by Matlab algorithm for quantification of angiogenesis in arteriovenous loop models. (Center, right) Nanofiber hydrogel composite with fractionated fat remodeled tissue exhibited a significantly higher total blood vessel count and a trend toward higher blood vessel cross-sectional area. (Below, right) Nanofiber hydrogel compound-only tissue exhibited a significant volume loss after 21 days of implantation compared to the intraoperative volume that had been implanted into the chamber, whereas the volume of nanofiber hydrogel composite with fractionated fat tissue did not change significantly. Scale bar = 1 mm. Schematic created with biorender.com.

into red, green, and blue channels, and each channel was converted to binary (using the imbinarize function) to determine the area covered by each

color. The 4',6-diamidino-2-phenylindole stain, corresponding to the blue channel, was thresholded on an image-specific level, automatically

determined from the function graythresh to optimize the number of 4',6-diamidino-2-phenylindole–stained cells counted on an image. To ensure observer independent quantification of the actual protein fluorescent levels, we converted images for the red and green channels to binary with a consistent threshold of 0.3 for all images of the same stain. The consistent threshold served to ensure unbiased quantification of the stain area. The area of red and green stains was then normalized by dividing by the number of individual blue (4',6-diamidino-2-phenylindole) objects, using the regionprops function.

Fractal Analysis

Fractal analysis was performed using the ImageJ (National Institutes of Health, Bethesda, Md.) plug-in FracLac.²⁰ Local fractal dimensions and lacunarity values were calculated using the subsample box counting scan (50 grid at default sampling size, minimum pixel density threshold = 0, subscan in rectangles).

Statistical Analysis

Statistical analysis was performed with GraphPad Prism 8 (GraphPad Software, Inc., San Diego, Calif.). Continuous variables were compared using an unpaired *t* test or the Mann-Whitney *U* test in case of non-Gaussian distribution. Normality was assessed using the Shapiro-Wilk test. Data are presented as means ± SEM or median and interquartile range, respectively. Values of *p* < 0.05 were considered statistically significant.

RESULTS

Vascularization

The implantation of an arteriovenous loop within the scaffolds induced the formation of a functional neovascular network within 21 days of implantation in both groups (Fig. 1, center, left, and below, left). We found that enrichment of nanofiber hydrogel composite with fractionated fat led to a significantly higher blood vessel count (mean, 833.5 ± 206.1 versus 296.5 ± 114.1; *p* = 0.04) (Fig. 1, center, right, and below, right, and Table 1) and a trend toward a higher mean vessel area (mean, 23,577 ± 5705 μm² versus 14,631 ± 4965 μm²; *p* = 0.26) (Fig. 1, center, right, and below, right, and Table 1) compared to nanofiber hydrogel composite alone. A stronger vascularization of nanofiber hydrogel composite with fractionated fat compared to nanofiber hydrogel composite

Table 1. Vascularization

	NHC	NHC-FF	<i>p</i>
Blood vessel area, μm ²	296.5 ± 114.1	833.5 ± 206.1	0.26*
Blood vessel count			
Total	14,631 ± 4965	23,577 ± 5705	0.04*
Center	82.0 ± 36.3	249.3 ± 74.5	0.07*
Periphery			0.24†
Median	97.0	160.7	
IQR	17.5–186.5	109.3–289.8	

NHC, nanofiber hydrogel composite; FF, fractionated fat; IQR, interquartile range.

**t* test.

†Mann-Whitney test.

alone was evident both in the central area around the main vessels (249.3 ± 74.5 versus 82.0 ± 36.3; *p* = 0.07) and in the periphery (208.8 ± 69.9 versus 102.0 ± 32.9; *p* = 0.24) (Table 1). Moreover, blood vessels within the nanofiber hydrogel composite with fractionated fat morphologically appeared as arterioles with a muscular tunica media and a collagenous adventitia as evident on Masson trichrome–stained sections. [See Figure, **Supplemental Digital Content 1**, which shows (left) histologic cross-sections of explanted nanofiber hydrogel composite (above) and nanofiber hydrogel composite with fractionated fat remodeled tissue at 21 days after implantation stained with Masson trichrome. Black boxes indicate the location of the magnified images in above left and below left. (Second from left, second from right, and right) A stronger vascularization of nanofiber hydrogel composite with fractionated fat–remodeled compared to nanofiber hydrogel composite alone was evident both in the central area around the main vessels (above, second from left, and above, second from right) and in the periphery (center, second from left, and center, second from right). Nanofiber hydrogel composite with fractionated fat–remodeled tissue appeared denser, with a significantly higher cell count (below, second from left, and below, second from right). Newly formed blood vessels within the nanofiber hydrogel composite with fractionated fat–remodeled tissue had differentiated into arterioles with a muscular tunica media and a collagenous adventitia (above, second from right). Arrowheads indicate ink-perfused functional blood vessels; arrow indicates adipocytes. Scale bar = 1 mm, <http://links.lww.com/PRS/E883>.]

Tissue Remodeling

Adipocytes, showing characteristic signet ring shapes, successfully engrafted into the nanofiber hydrogel composite with fractionated fat tissue, which demonstrated a striking similarity to native mammalian subdermal tissue.

Emulsification of fractionated fat also resulted in dispersion of oil droplets from burst adipocytes within the nanofiber hydrogel composite, which showed a more irregularly shaped histologic appearance (Fig. 1 center, left and below, left). [See Figure, Supplemental Digital Content 1, <http://links.lww.com/PRS/E883>. See Figure, Supplemental Digital Content 2, which shows histologic cross-sections of explanted nanofiber hydrogel composite with fractionated fat tissue at 21 days after implantation stained with Masson trichrome. Black boxes indicate the location of the magnified images showing irregularly shaped oil droplets from emulsification of fractionated fat (below, left) and engrafted signet ring-shaped adipocytes (below, right). Scale bar = 1 mm, <http://links.lww.com/PRS/E884>.] Remodeling and cellular infiltration in nanofiber hydrogel composite-only tissue was restricted to an area immediately surrounding the main loop vessels, whereas large parts of the chamber content remained acellular and avascular (Fig. 1, center, left, and below, left). By contrast, nanofiber hydrogel composite with fractionated fat tissue showed a strong remodeling of the entire chamber content and a 5.4-fold higher cell count (mean cell count per cross-section, $49,707 \pm 18,491$ versus 9263 ± 3790 ; $p = 0.005$). At the time of explantation, nanofiber hydrogel composite-only tissue exhibited a volume reduction by 88 percent compared to the intraoperative chamber volume ($0.18 \pm 0.02 \text{ cm}^3$ versus 0.8 cm^3 ; $p < 0.0001$), whereas nanofiber hydrogel composite with fractionated fat tissue maintained its shape without shrinking significantly ($0.63 \pm 0.04 \text{ cm}^3$) (Fig. 1, below, right).

As the complex patterns of dermal and subdermal soft tissue cannot be described with traditional Euclidean geometry, we performed fractal analysis to compare the histologic architecture between nanofiber hydrogel composite and nanofiber hydrogel composite with fractionated fat tissue. Fractal analysis applies nontraditional mathematics to complex patterns that defy understanding with traditional Euclidean geometry. The fractal dimension defines the overall complexity of a shape, whereas lacunarity represents the rotational and translational invariance as a measure of gaps and heterogeneity. Although we did not find a difference in overall tissue complexity with similar fractal dimension values in nanofiber hydrogel composite and nanofiber hydrogel composite with fractionated fat tissues, the nanofiber hydrogel composite with fractionated fat demonstrated a significantly stronger heterogeneity (lacunarity)

(mean lacunarity score, 0.42 ± 0.01 versus 0.36 ± 0.002 ; $p = 0.03$) (Fig. 2).

Protein Expression

We further compared the expression of regenerative and proliferation markers using immunofluorescent staining and confocal laser scanning microscopy of tissue sections. We found a significantly higher expression of CD34, a marker for mesenchymal stem cells, in nanofiber hydrogel composite with fractionated fat compared to nanofiber hydrogel composite tissue (CD34⁺ area/4',6-diamidino-2-phenylindole, 0.45 ± 0.03 versus 0.22 ± 0.06 ; $p = 0.01$) (Fig. 3 and Table 2).

The majority of cells infiltrating the tissue were macrophages, expressing the panmacrophage marker CD68 (CD68⁺ area/4',6-diamidino-2-phenylindole, 0.82 ± 0.17 versus 0.62 ± 0.27 ; $p = 0.54$). While nanofiber hydrogel composite alone exhibited an even distribution of macrophages within the tissue (Table 2), we found that macrophages were aligned around oil droplets in nanofiber hydrogel composite with fractionated fat remodeled tissue, a phenomenon that has recently been described for regenerative lipid associated macrophages.²¹ [See Figure, Supplement Digital Content 3, which shows immunofluorescent staining for CD68 (panmacrophage marker), indicating that the majority of cells infiltrating the scaffolds were macrophages. Macrophages were organized around oil droplets in nanofiber hydrogel composite with fractionated fat (NHC-FF)-remodeled tissue (below) and more evenly distributed in the nanofiber hydrogel composite (NHC) implants (above). Yellow boxes indicate the location of the magnified areas. Arrows indicate CD68+ cells within the tissue. Scale bar = 1 mm, <http://links.lww.com/PRS/E885>.]

To further characterize regenerative macrophage subpopulations, we performed immunofluorescent staining for CD163 (hemoglobin scavenger receptor) and found a nearly 20 times higher number of CD163⁺ cells in nanofiber hydrogel composite with fractionated fat-remodeled tissue compared to nanofiber hydrogel composite implant alone (946.7 ± 273.6 cells versus 47.5 ± 19.42 cells; $p = 0.02$) (Fig. 4 and Table 2).

DISCUSSION

For decades, tissue engineering approaches have aimed to develop alternative solutions to restore soft-tissue defects without the need for autologous tissue transfer.^{13,22} The main challenge for reconstruction of soft-tissue defects with

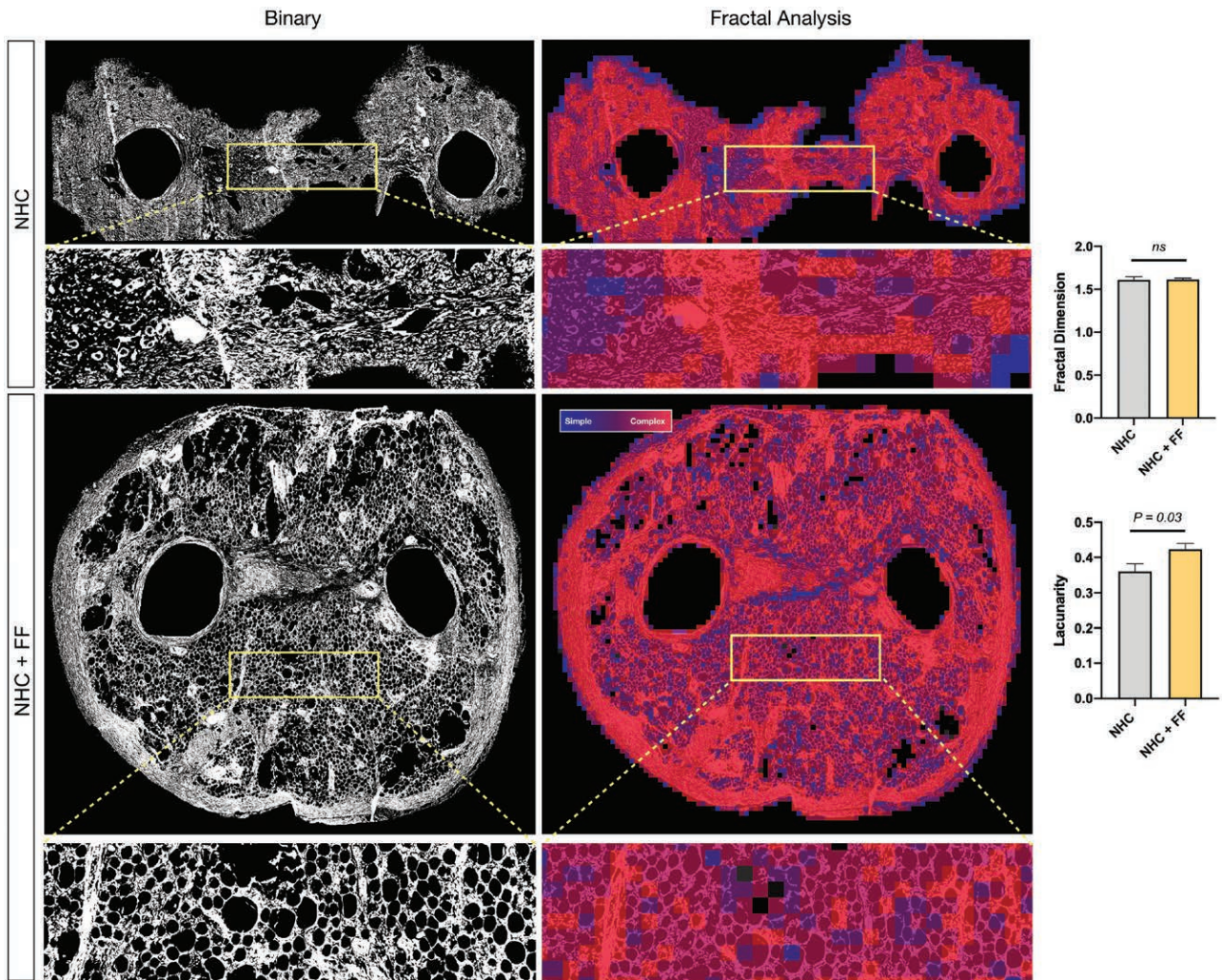


Fig. 2. Fractal analysis of tissue remodeled with nanofiber hydrogel composite (NHC) (above) and nanofiber hydrogel composite with fractionated fat (NHC+FF) (below). The overall tissue complexity was comparable between the groups as indicated by similar fractal dimension scores. In nanofiber hydrogel composite with fractionated fat-remodeled tissue, fractionated fat induced a significantly higher heterogeneity (lacunarity) as evidence for stronger tissue remodeling. Yellow boxes indicate the magnified areas. White dotted lines indicate the arteriovenous loop main vessels. Scale bar = 1 mm.

acellular scaffolds is adequate vascularization.¹³ Neoangiogenesis and blood vessel ingrowth into acellular materials requires days to weeks and thus may fail to provide a timely supply of oxygen and nutrients to allow for viable host tissue ingrowth if large volumes of acellular scaffolds are implanted.^{23,24} Thus, strategies of regenerative medicine to promote angiogenesis within these materials are of critical importance for the development of minimally invasive approaches that might eventually be used to restore large soft-tissue defects without the risk for donor-site morbidity.

We have recently developed a nanofiber hydrogel composite that mimics the microarchitecture of native extracellular matrix with the biomechanical properties of human adipose tissue.¹¹

This hydrogel promotes host cellular infiltration and is gradually replaced by native soft tissue.¹⁰ The development of nanofat and fractionated fat has shown great benefit for the restoration of age-related soft-tissue damage in aesthetic surgery.^{6,7} However, only a few studies have leveraged the potential of fractionated fat to enhance the vascularization of biological scaffolds for the purpose of tissue engineering in reconstructive surgery.^{25,26}

Here, we developed a novel approach for tissue engineering of vascularized soft tissue by using the synergistic effect of fractionated fat in combination with our established nanofiber hydrogel composite. To analyze the potential of our novel nanofiber hydrogel composite with fractionated fat scaffold to induce a functional neovasculature,

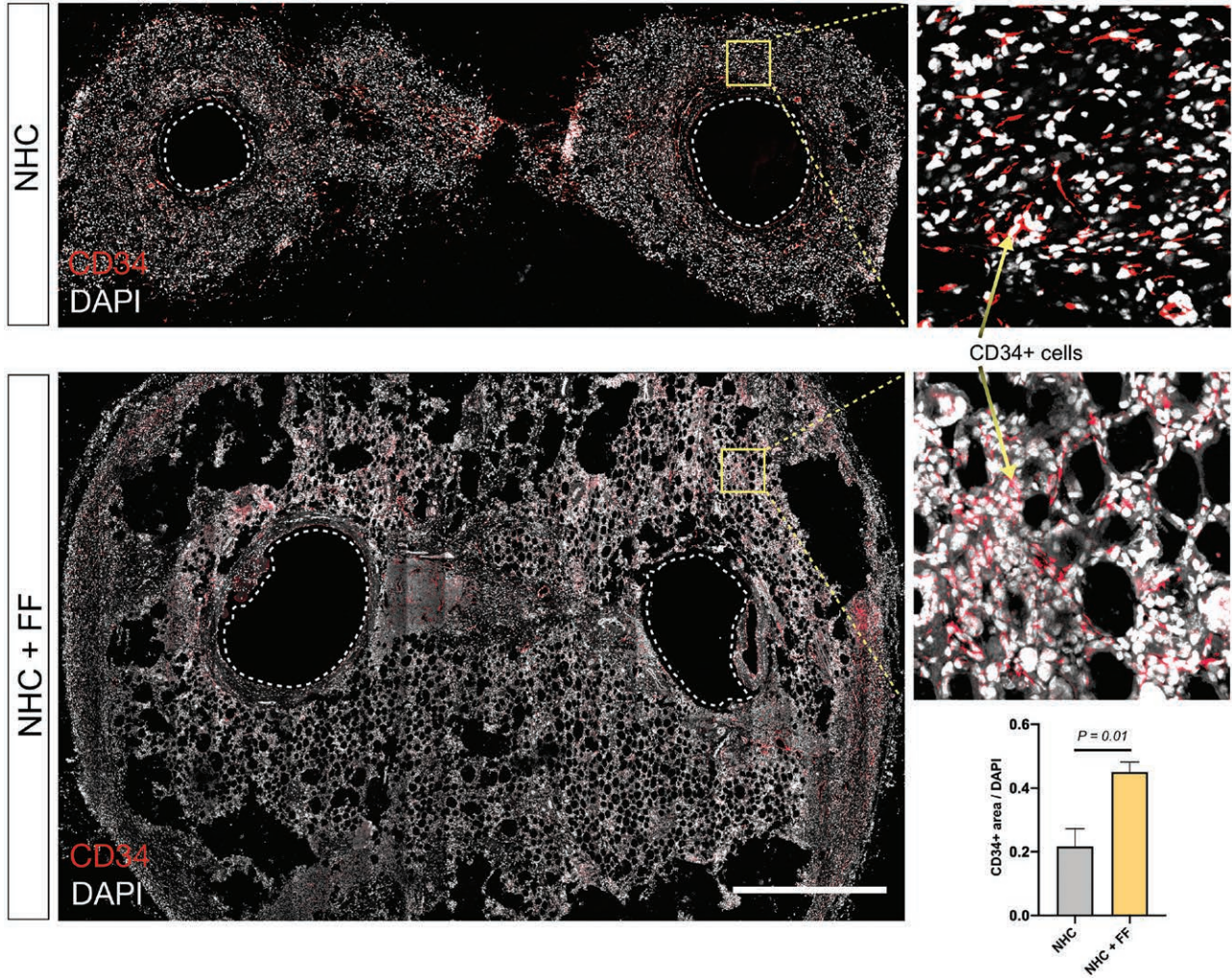


Fig. 3. Immunofluorescent staining for CD34 (progenitor cell marker) indicated a significantly higher proportion of CD34⁺ cells in nanofiber hydrogel composite with fractionated fat (NHC-FF)-remodeled tissue (below) compared to nanofiber hydrogel composite (NHC) (above). Yellow boxes indicate the location of the magnified areas. Arrows indicate CD34⁺ cells within the tissue. DAPI, 4',6-diamidino-2-phenylindole.

we used the arteriovenous loop model, which was first described by Melvin Spira’s group in 1979 and has since been developed into a standard model for the investigation of blood vessel development in vivo without the need for externally applied growth factors.^{13,27–29}

Enrichment of nanofiber hydrogel composite with fractionated fat led to a significantly stronger vascularization compared to nanofiber

hydrogel composite alone and maintained its shape without shrinking over 21 days of in vivo implantation. In nanofiber hydrogel composite with fractionated fat-remodeled tissue, functional ink-perfused blood vessels were evenly distributed and reached the periphery of the tissue, whereas blood vessels in the periphery of nanofiber hydrogel composite tissue without fractionated fat were sparse. Moreover, fractionated fat induced a significantly stronger tissue heterogeneity, which was quantified by fractal analysis of the tissue microarchitecture. The higher lacunarity of the nanofiber hydrogel composite with fractionated fat-remodeled tissue is likely related to the engraftment of adipocytes and dispersion of oil droplets within the engineered soft tissue, which led to a striking histologic similarity with native mammalian

Table 2. Protein Expression

	NHC	NHC-FF	<i>p</i> *
CD34, area/cell	0.22 ± 0.06	0.45 ± 0.03	0.01
CD68, area/cell	0.62 ± 0.27	0.82 ± 0.17	0.54
CD163, cell count	47.5 ± 19.42	946.7 ± 273.6	0.02

NHC, nanofiber hydrogel composite; FF, fractionated fat.

**t* test.

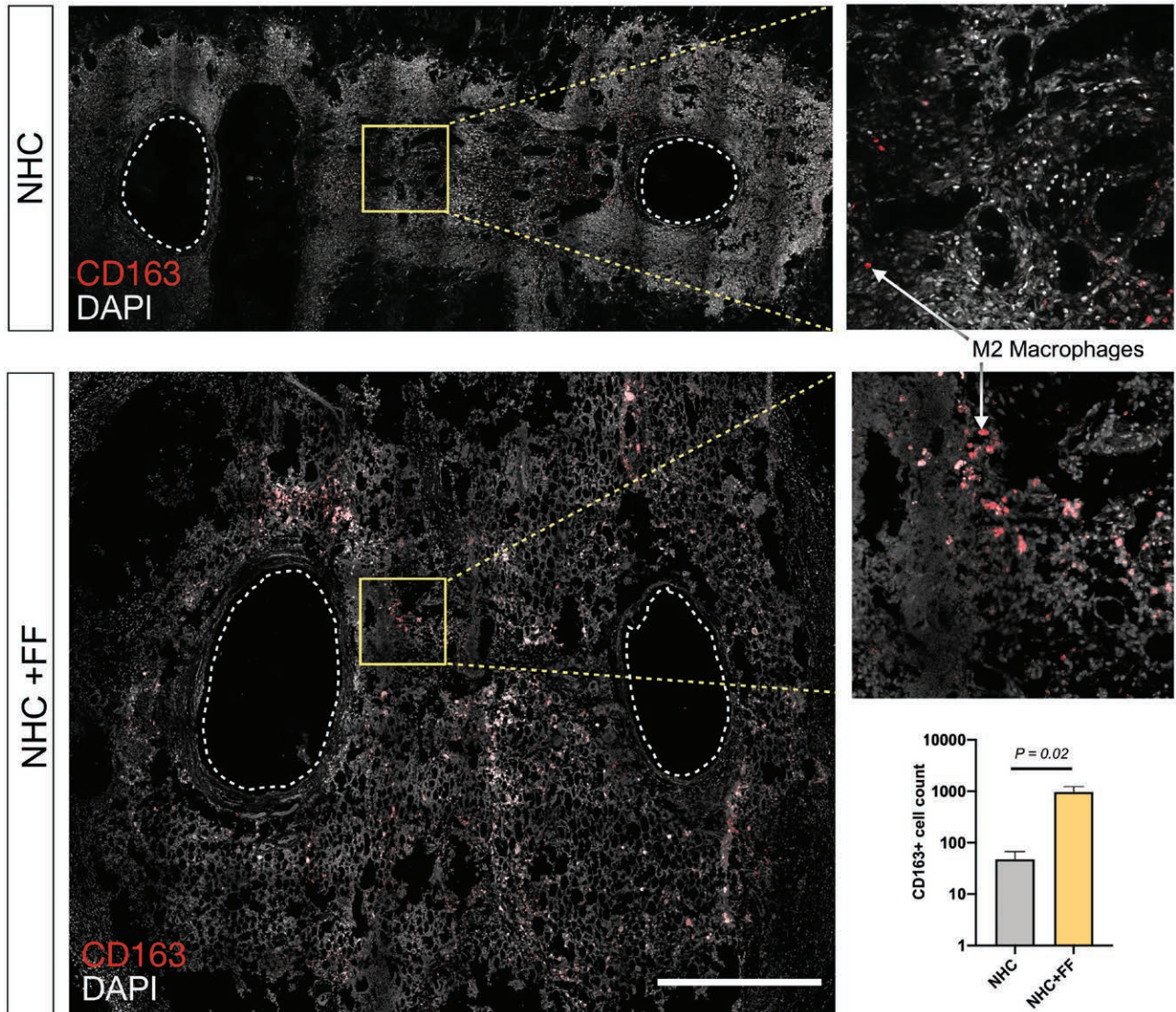


Fig. 4. Immunofluorescent staining for CD163 (regenerative macrophage marker) indicated a significantly higher amount of CD163⁺ cells in nanofiber hydrogel composite with fractionated fat–remodeled tissue (*below*) compared to nanofiber hydrogel composite alone (*above*). Yellow boxes indicate the location of the magnified areas. Arrows indicate CD163⁺ cells within the tissue. Scale bar = 1 mm.

subdermal tissue (Fig. 1 and Figure, Supplemental Digital Content 1, <http://links.lww.com/PRS/E883>).

We found a significantly higher proportion of CD34⁺ cells in nanofiber hydrogel composite with fractionated fat–remodeled tissue compared to nanofiber hydrogel composite alone, which indicates that the mesenchymal stem cells derived from the fractionated fat engraft into the nanofiber hydrogel composite and are still highly abundant after 21 days of implantation, which might be the cause of the observed sustained regenerative and proangiogenic effects.

As we have previously shown that nanofiber hydrogel composite promotes host macrophage

infiltration, we aimed to assess whether our novel nanofiber hydrogel with fractionated fat composite has an impact on regenerative macrophage phenotypes. We did not find significant differences in overall macrophage infiltration into the tissue; however, we found that macrophages accumulated around oil droplets in nanofiber hydrogel composite with fractionated fat–remodeled tissue. This pattern may represent a lipid-associated macrophage phenotype that has recently been shown to have a robust regenerative and antiinflammatory capacity.²¹ However, further studies are necessary to more accurately classify macrophage subpopulations

infiltrating nanofiber hydrogel composite and nanofiber hydrogel composite with fractionated fat scaffolds.

Moreover, we quantified the amount of macrophages expressing the hemoglobin scavenger receptor CD163, a characteristic marker for regenerative M2-like macrophages,³⁰ which has recently been associated with a perivascular macrophage subpopulation critically involved in wound healing and tissue repair.³¹ Significantly higher numbers of CD163⁺ macrophages were found in nanofiber hydrogel composite with fractionated fat–remodeled tissue compared to nanofiber hydrogel composite alone, indicating the strong regenerative capacity of the fractionated fat and its potential for tissue engineering of vascularized soft tissue. The process of fat fragmentation may lead to red blood cell lysis and an increase in free hemoglobin, which might serve as a trigger for CD163 expression within macrophages in the nanofiber hydrogel composite with fractionated fat scaffold.

Several studies in small- and large-animal models have demonstrated that the arteriovenous loop model is a useful tool for *in vivo* expansion of native adipose tissue flaps,^{32–34} indicating that fat can serve as a scaffold for tissue engineering in this model. Debels et al. have compared processed fat alone with a composite material consisting of an adipose-derived acellular matrix enriched with fat as a scaffold for arteriovenous loop–based tissue engineering and demonstrated that the combination of an acellular scaffold with viable fat significantly enhances the regenerative process.³⁵ Fractionated fat has been shown to improve wound healing in diabetic rats and photoaging in nude mice, indicating its merit for regenerative medicine.^{25,26} Huang et al. used nanofat in conjunction with ceramic granules to promote chondrogenic differentiation of mesenchymal progenitor cells, further highlighting the potential of nanofat/fractionated fat for bone tissue engineering.³⁶ Our study is the first to use fractionated fat to enhance the vascularization of a nanofiber hydrogel scaffold for soft-tissue engineering. The approach we present has several advantages, which may facilitate future clinical translation. Fractionated fat can easily be obtained from lipoaspirate in the operating room by mechanical emulsification of fat with two syringes and a Luer-lock connector using clinically established protocols.⁷ The nanofiber hydrogel composite is designed to be an off-the-shelf product and effectively guides cellular infiltration along

its nanofibers. Moreover, the nanofiber hydrogel composite itself promotes angiogenesis and exhibits the biomechanical properties of human soft tissue.^{10,29} The synergistic combination of fractionated fat with the unique architecture of the nanofiber hydrogel composite allowed us to develop a technique for engineering of soft tissue with an enhanced regenerative remodeling, more robust vascularization, and better shape maintenance.

Limitations of our study are mainly related to its sample size, which, however, is comparable to previously published studies investigating *in vivo* soft-tissue engineering.^{23,24,37} We chose to explant the tissue on postoperative day 21, because the vascularization of arteriovenous loop constructs have been shown to be sufficient for free transplantation and defect coverage as early as postoperative day 14 using the main loop vessels as a pedicle.²³ During this relatively short implantation period, the nanofiber hydrogel composite with fractionated fat composite induced a rapid vascularization, cellular infiltration, and neotissue formation throughout the entire remodeled construct, in contrast to previously published techniques using isolation chambers, which show large avascular and acellular areas.^{24,28,29} Changes in vascularization and tissue remodeling of our nanofiber hydrogel with fractionated fat composite over longer implantation periods are an interesting subject for investigation in future studies.

We cannot exclude the presence of small vascular and lymphatic structures within the transplanted fractionated fat. Therefore, our current study does not conclusively discriminate between blood vessels that developed as a result of neovascular sprouting from the arteriovenous loop and vessels that preexisted within the transplanted fat, which were revascularized in the chamber through the process of inosculation.³⁸ Nevertheless, we have used a clinically established approach for fat processing⁷ to develop a novel technique that improves the vascularization of scaffold-based tissue engineered constructs, and thus believe that our findings have a high potential for clinical translation. Future studies have to investigate how vascularization and tissue remodeling of the nanofiber hydrogel composite with fractionated fat compares to fractionated fat alone and whether the improved vascularization observed after transplantation of fractionated fat mainly results from inosculation or neoangiogenesis.

CONCLUSIONS

Enrichment of nanofiber-hyaluronic acid hydrogel composite with fractionated fat represents a promising approach for engineering soft tissue with a robust vascularization, cell engraftment, and infiltration of regenerative macrophages. Our approach may ultimately lay the groundwork for clinically relevant applications, with the goal of generating vascularized soft tissue for defect reconstruction without the need for autologous tissue transfer.

Justin M. Sacks, M.D., M.B.A.

Division of Plastic and Reconstructive Surgery
Department of Surgery
Washington University in St. Louis School of Medicine
660 South Euclid Avenue
St. Louis, Mo. 63110
jmsacks@wustl.edu

ACKNOWLEDGMENTS

The microscopy and imaging performed in this study were supported by the Cell Sciences Imaging Facility and the Beckman Foundation at Stanford University.

REFERENCES

- Piccolo NS, Piccolo MS, Piccolo MT. Fat grafting foq2r treatment of burns, burn scars, and other difficult wounds. *Clin Plast Surg*. 2015;42:263–283.
- Luu CA, Larson E, Rankin TM, Pappalardo JL, Slepian MJ, Armstrong DG. Plantar fat grafting and tendon balancing for the diabetic foot ulcer in remission. *Plast Reconstr Surg Glob Open* 2016;4:e810.
- Coleman SR. Structural fat grafting: More than a permanent filler. *Plast Reconstr Surg*. 2006;118(Suppl):108S–120S.
- Zuk PA, Zhu M, Mizuno H, et al. Multilineage cells from human adipose tissue: Implications for cell-based therapies. *Tissue Eng*. 2001;7:211–228.
- Tonnard P, Verpaele A, Peeters G, Hamdi M, Cornelissen M, Declercq H. Nanofat grafting: Basic research and clinical applications. *Plast Reconstr Surg*. 2013;132:1017–1026.
- Tonnard P, Verpaele A, Carvas M. Fat grafting for facial rejuvenation with nanofat grafts. *Clin Plast Surg*. 2020;47:53–62.
- Rohrich RJ, Mahedia M, Shah N, Afroz P, Vishvanath L, Gupta RK. Role of fractionated fat in blending the lid-cheek junction. *Plast Reconstr Surg*. 2018;142:56–65.
- Kanchwala SK, Bucky LP. Facial fat grafting: The search for predictable results. *Facial Plast Surg*. 2003;19:137–146.
- Lee KT, Kim A, Mun GH. Comprehensive analysis of donor-site morbidity following free thoracodorsal artery perforator flap harvest. *Plast Reconstr Surg*. 2016;138:899–909.
- Li X, Cho B, Martin R, et al. Nanofiber-hydrogel composite-mediated angiogenesis for soft tissue reconstruction. *Sci Transl Med*. 2019;11:eaau6210.
- Henn D, Chen K, Fischer K, et al. Tissue engineering of axially vascularized soft-tissue flaps with a poly-(ϵ -caprolactone) nanofiber-hydrogel composite. *Adv Wound Care (New Rochelle)* 2020;9:365–377.
- Messina A, Bortolotto SK, Cassell OC, Kelly J, Abberton KM, Morrison WA. Generation of a vascularized organoid using skeletal muscle as the inductive source. *FASEB J*. 2005;19:1570–1572.
- Leibig N, Wietbrock JO, Bigdeli AK, et al. Flow-induced axial vascularization: The arteriovenous loop in angiogenesis and tissue engineering. *Plast Reconstr Surg*. 2016;138:825–835.
- Pitt CG, Gratzl MM, Kimmel GL, Surles J, Schindler A. Aliphatic polyesters II. The degradation of poly (DL-lactide), poly (epsilon-caprolactone), and their copolymers in vivo. *Biomaterials* 1981;2:215–220.
- Woodward SC, Brewer PS, Moatamed F, Schindler A, Pitt CG. The intracellular degradation of poly(epsilon-caprolactone). *J Biomed Mater Res*. 1985;19:437–444.
- Polykandriotis E, Tjjiawi J, Euler S, et al. The venous graft as an effector of early angiogenesis in a fibrin matrix. *Microvasc Res*. 2008;75:25–33.
- Weis C, Covi JM, Hilgert JG, et al. Automatic quantification of angiogenesis in 2D sections: A precise and timesaving approach. *J Microsc*. 2015;259:185–196.
- Chen K, Vigliotti A, Bacca M, McMeeking RM, Deshpande VS, Holmes JW. Role of boundary conditions in determining cell alignment in response to stretch. *Proc Natl Acad Sci USA*. 2018;115:986–991.
- Henn D, Chen K, Maan ZN, et al. Cryopreserved human skin allografts promote angiogenesis and dermal regeneration in a murine model. *Int Wound J*. 2020;17:925–936.
- Kam Y, Karperien A, Weidow B, Estrada L, Anderson AR, Quaranta V. Nest expansion assay: A cancer systems biology approach to in vitro invasion measurements. *BMC Res Notes* 2009;2:130.
- Jaitin DA, Adlung L, Thaiss CA, et al. Lipid-associated macrophages control metabolic homeostasis in a Trem2-dependent manner. *Cell* 2019;178:686–698.e14.
- Horch RE, Kneser U, Polykandriotis E, Schmidt VJ, Sun J, Arkudas A. Tissue engineering and regenerative medicine: Where do we stand? *J Cell Mol Med*. 2012;16:1157–1165.
- Schmidt VJ, Wietbrock JO, Leibig N, et al. Haemodynamically stimulated and in vivo generated axially vascularized soft-tissue free flaps for closure of complex defects: Evaluation in a small animal model. *J Tissue Eng Regen Med*. 2018;12:622–632.
- Schmidt VJ, Wietbrock JO, Leibig N, et al. Collagen-elasticity and collagen-glycosaminoglycan scaffolds promote distinct patterns of matrix maturation and axial vascularization in arteriovenous loop-based soft tissue flaps. *Ann Plast Surg*. 2017;79:92–100.
- Zheng H, Qiu L, Su Y, Yi C. Conventional nanofat and SVF/ADSC-concentrated nanofat: A comparative study on improving photoaging of nude mice skin. *Aesthet Surg J*. 2019;39:1241–1250.
- Chen L, Wang ZC, Ma JJ, et al. Autologous nanofat transplantation accelerates foot wound healing in diabetic rats. *Regen Med*. 2019;14:231–241.
- Erol OO, Sira M. New capillary bed formation with a surgically constructed arteriovenous fistula. *Plast Reconstr Surg*. 1980;66:109–115.
- Henn D, Abu-Halima M, Falkner F, et al. Micro-RNA-regulated proangiogenic signaling in arteriovenous loops in patients with combined vascular and soft-tissue reconstructions: Revisiting the nutrient flap concept. *Plast Reconstr Surg*. 2018;142:489e–502e.
- Henn D, Chen K, Fischer K, et al. Tissue engineering of axially vascularized soft-tissue flaps with a poly-(ϵ -caprolactone) nanofiber-hydrogel composite. *Adv Wound Care (New Rochelle)* 2020;9:365–377.
- Krzyszczak P, Schloss R, Palmer A, Berthiaume F. The role of macrophages in acute and chronic wound healing and interventions to promote pro-wound healing phenotypes. *Front Physiol*. 2018;9:419.

31. Chakarov S, Lim HY, Tan L, et al. Two distinct interstitial macrophage populations coexist across tissues in specific subtissular niches. *Science* 2019;363:eaau0964.
32. Findlay MW, Dolderer JH, Trost N, et al. Tissue-engineered breast reconstruction: Bridging the gap toward large-volume tissue engineering in humans. *Plast Reconstr Surg*. 2011;128:1206–1215.
33. Yap KK, Yeoh GC, Morrison WA, Mitchell GM. The vascularised chamber as an in vivo bioreactor. *Trends Biotechnol*. 2018;36:1011–1024.
34. Morrison WA, Marre D, Grinsell D, Batty A, Trost N, O'Connor AJ. Creation of a large adipose tissue construct in humans using a tissue-engineering chamber: A step forward in the clinical application of soft tissue engineering. *EBioMedicine* 2016;6:238–245.
35. Debels H, Palmer J, Han XL, Poon C, Abberton K, Morrison W. In vivo tissue engineering of an adipose tissue flap using fat grafts and Adipogel. *J Tissue Eng Regen Med*. 2020;14:633–644.
36. Huang RL, Guerrero J, Senn AS, et al. Dispersion of ceramic granules within human fractionated adipose tissue to enhance endochondral bone formation. *Acta Biomater*. 2020;102:458–467.
37. Steiner D, Lingens L, Fischer L, et al. Encapsulation of mesenchymal stem cells improves vascularization of alginate-based scaffolds. *Tissue Eng Part A* 2018;24:1320–1331.
38. Capla JM, Ceradini DJ, Tepper OM, et al. Skin graft vascularization involves precisely regulated regression and replacement of endothelial cells through both angiogenesis and vasculogenesis. *Plast Reconstr Surg*. 2006;117:836–844.